magnetism

MDPI

Article

Correlation of Light Polarization in the Magnetic Media with Non-Spherical Point-like Inclusions

Ramil A. Niyazov [1,2]*, Venu Gopal Achanta [3] and Vladimir I. Belotelov [4,5]

[1] Department of Physics, St. Petersburg State University, St. Petersburg 198504, Russia
[2] Petersburg Nuclear Physics Institute, NRC "Kurchatov Institute", Gatchina 188300, Russia
[3] Tata Institute of Fundamental Research, Mumbai 400005, India
[4] Russian Quantum Center, Skolkovskoe Shosse 45, Moscow 121353, Russia
[5] Faculty of Physics, Lomonosov Moscow State University, Leninskie Gory 1, Moscow 119991, Russia
* Correspondence: r.niyazov@spbu.ru

Abstract: Light propagation through magnetic media with ellipsoidal inclusions much smaller than the light wavelength was investigated theoretically. It is assumed that the ellipsoidal inclusions have the same orientation but are randomly distributed inside the magnetic medium by the Gaussian law. The theoretical model is based on the multiple-scattering theory in the ladder approximation. A new type of electromagnetic field correlation is found to appear in this case, while it is absent in isotropic magnetic nanocomposites and nonmagnetic anisotropic composites. This feature allows for the precise control of light polarization in anisotropic magnetic media.

Keywords: magneto-optical effects; disordered media; electric field correlation matrix; multiple-scattering theory

Citation: Niyazov, R.A.; Achanta, V.G.; Belotelov, V.I. Correlation of Light Polarization in the Magnetic Media with Non-Spherical Point-like Inclusions. *Magnetism* **2023**, *3*, 1–10. https://doi.org/10.3390/magnetism3010001

Academic Editors: Efrat Lifshitz and Victor M. de la Prida Pidal

Received: 12 July 2022
Revised: 3 November 2022
Accepted: 14 December 2022
Published: 29 December 2022

1. Introduction

Light propagation in scattering media is relevant to different disciplines, ranging from chemistry and biology to astronomy and physics [1]. The fast-evolving field of nanophotonics is directly connected to light propagation through nanostructured materials [2]. Nowadays, light propagation in disordered media is being actively investigated in theory [3–7] and experiments [8–10]. In disordered media, the fluctuation in the scattered-light component depends on disorder. The description of such fluctuation is based on statistical approaches [11]. The theory of polarization and the coherence of random electromagnetic fields was formulated in Ref. [12]. Within this theory, it is possible to compute the degree of polarization and coherence and the spectrum of light during the beam propagation [13]. Light localization is one of the hot topics, with considerable literature devoted to the weak localization and the Anderson localization of light in the scattering media [14–18].

Recently, polarization effects in non-magnetic disordered media were intensively studied using the multiple-scattering theory in terms of "polarization eigenmodes" [19,20]. The magnetization of the scattering media leads to the emergence of a wide class of effects. Among them, there are the photonic Hall effect in magnetic media [21], the coherent backscattering suppression by the field [22], and the magnetic-field-driven light localization in a cold atom gas [23]. Likewise, magneto-optical effects are studied in the framework of the multiple-scattering theory. Research on magneto-active media with point-like inclusions [24,25] and non-magnetic media with magneto-optical scatterers [26] has been carried out. The approach of "polarization eigenmodes" was used to analyze magneto-active media [27]. A correlation between orthogonal light polarizations at a scale of several wavelengths was demonstrated earlier in an uncorrelated disordered magnetic media with spherical scatterers [28].

Special attention is paid to the creation and study of anisotropic materials. They begin to have new features because the anisotropy breaks the symmetry and allows one to create

increasingly complex structures [29]. For example, anisotropy can remove the degeneracy of the photonic band structure leading to partial band gaps [30]. Nanocomposite systems with anisotropic inclusions can be created within self-organized structures with distributions of nanoparticles in the bulk of the eutectic composite [31] and by the directed self-assembly of the nanoparticles method [32].

It turns out that the presence of the three above-mentioned phenomena in the material (magnetoactivity, disorder, and anisotropy) leads to rich possibilities for controlling the polarization of light. In this work, we investigate the correlation of light polarization in a nanocomposite medium consisting of nonmagnetic nanoparticles of an ellipsoidal shape in a magnetic dielectric matrix (Figure 1). We assume the Gaussian model for the disorder, where scatterers are distributed randomly and their size is negligible compared to the wavelength of light. We also considered that the ellipsoid axes are aligned with each other. Additionally, we assume that the ellipsoid has two equal semi-diameters, a spheroid. Such ellipticity leads to the uniaxial anisotropy of the dielectric tensor.

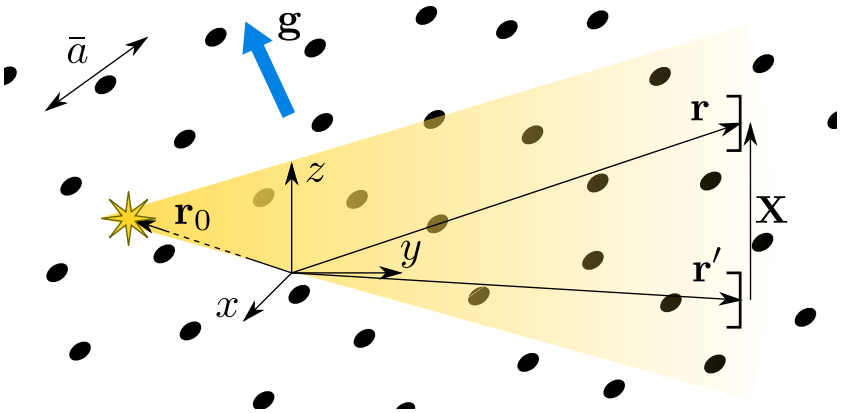

Figure 1. Schematic representation of the light propagation from a source at a point $\mathbf{r}_0$ inside an infinite magnetic nanocomposite medium with a gyration $\mathbf{g}$ containing scatterers with an anisotropy axis $\bar{a}$. Electromagnetic field detectors are placed at points $\mathbf{r}$ and $\mathbf{r}'$, $\mathbf{X} \equiv \mathbf{r} - \mathbf{r}'$.

A similar model can be implemented in materials based on a dilute three-dimensional colloidal suspension of randomly arranged anisotropic particles. In this case, the collective alignment of ellipsoidal particles and the anisotropy control can be carried out by external electric [29] or magnetic [33] fields. Additionally, similar systems can be created by the method of layering self-organized material with the annealing of matrix material [34]. In this paper there was no focus on the anisotropy of inclusions; therefore, this issue was not investigated, but the presence of a defect in the form of a surface during the growth of such systems should lead to the alignment of the axes of the ellipsoid.

Let us consider a point-dipole light source, at point $\mathbf{r}_0$, located far from the observation points $\mathbf{r}$ and $\mathbf{r}'$. The correlation of electromagnetic fields with different polarizations at the observation points is described by the field correlation matrix $W_{kl}(\mathbf{r}, \mathbf{r}') = \langle E_k(\mathbf{r}) E_l^*(\mathbf{r}') \rangle$ [35], where $\langle \ldots \rangle$ means the ensemble average over the realizations of the field. It contains information on the interconnection between electromagnetic waves at two distinct points averaged over all possible disorder realizations. For example, the element W_{xx} characterizes how the light polarized along the $x-$ axis at the point $\mathbf{r}$, $E_x(\mathbf{r})$, is correlated to the light with the same polarization at the point $\mathbf{r}'$, $E_x(\mathbf{r}')$. The elements of the correlation matrix, $\mathbf{W}$, can be measured in Young's interference experiments [36]. They describe radiation, propagation, diffraction, and the interference of light [37].

The effect of magnetization on the optical properties of a medium is described by means of magneto-optical effects. In magnetic media with scattering particles, the correlation of orthogonal electric fields emerges. This occurs in the plane that is perpendicular to the gyration vector, $\mathbf{g}$, that is used to describe the magneto-optical effects. Gyration is proportional to the magnetization in the medium and contributes to the off-diagonal terms

in the dielectric tensor. For example, when $\mathbf{g} \parallel z$ the correlation of $E_x(\mathbf{r})$ and $E_y(\mathbf{r}')$, W_{xy}, arises. Moreover, if the scattering particles are isotropic then we have the antisymmetric correlation, $W_{yx} = -W_{xy}$, which corresponds to the circularly polarized part of the scattered light. Namely, if the initial light polarization $E_y(\mathbf{r})$ has the antisymmetric correlation with the final polarization $E_x(\mathbf{r}')$ then the initial polarization $E_x(\mathbf{r})$ correlates with the final polarization $E_y(\mathbf{r}')$ with the opposite sign of the correlation, which corresponds to the circular polarization.

The anisotropy of scattering particles in magnetic media leads to the emergence of the symmetric off-diagonal correlation matrix terms, which is one of the main results of this article. It corresponds to the emergence of ellipticity in the polarization. One can smoothly vary the character of polarization from circular to ellipsoidal and further to linear by changing the ratio of the gyration and anisotropy.

2. Effective Dielectric Tensor

We use the multiple-scattering theory, an ab initio approach, to describe the light propagation in the disordered media [38,39]. The electric field obeys the Helmholtz equation:

$$(\nabla \times \nabla - \hat{\epsilon} k_0^2)\mathbf{E} = i\mu_0 \omega \mathbf{j}, \tag{1}$$

where $k_0 = 2\pi/\lambda$ is the light wavevector in vacuum, λ is the light wavelength, $\mathbf{j}$ is the current density of the light source, and $\hat{\epsilon} = \hat{\epsilon}(\mathbf{r})$ is the dielectric tensor of the nanocomposite medium. We assume that the light source is a point dipole with a dipole moment $p = 1/\mu_0\omega^2$ located at $\mathbf{r}_0$ and oriented along the ℓ-th axis:

$$j_i(\mathbf{r}, \mathbf{r}_0) = -i\omega p \delta_{i\ell} \delta(\mathbf{r} - \mathbf{r}_0). \tag{2}$$

In the case of the magnetic media without the disorder, the dielectric tensor does not depend on $\mathbf{r}$ and has the following form:

$$\epsilon_{ij} = \epsilon^0 \delta_{ij} - \sum_{k=x,y,z} i e_{ijk} g_k. \tag{3}$$

Here, δ_{li} is the Kronecker Delta, ϵ^0 is the diagonal part of the dielectric tensor, and e_{ijk} is the Levi–Civita tensor.

Impurities in the media may be considered as fluctuations of the dielectric tensor $\delta\hat{\epsilon}(\mathbf{r})$. Fluctuations in the case of an isotropic uncorrelated disorder are as follows: $\delta\epsilon_{ij}(\mathbf{r}) = \delta_{ij}\delta\epsilon(\mathbf{r})$. Here, we consider anisotropic impurities. In accordance with the white noise model [39], the dielectric tensor of the medium has the following form:

$$\begin{aligned} \delta\epsilon_{ij}(\mathbf{r}) &= \delta_{ij}(1 + a_j)\delta\epsilon(\mathbf{r}), \\ \langle \delta\epsilon(\mathbf{r}) \rangle = 0, \quad \langle \delta\epsilon(\mathbf{r}) \delta\epsilon(\mathbf{r}') \rangle &= \frac{6\pi}{l(\epsilon^0 k_0^2)^2} \delta(\mathbf{r} - \mathbf{r}'), \end{aligned} \tag{4}$$

where a_j is an anisotropy parameter aligned with the j-th axis, $\langle \ldots \rangle$ means averaging over the Gaussian distributed disorder, and l is the scattering elastic mean free path of photons in a medium. Further, we consider the uniaxially anisotropic disorder such that a_j is non-zero along only one axis $\bar{a}$ with value a.

We solve the Helmholtz Equation (1) in the Bourret approximation [40], $\zeta \equiv 1/\sqrt{\epsilon^0} k_0 l \ll 1$, and the low anisotropy approximation $a \ll 1$. Additionally, we compute the effective dielectric tensor, ϵ_{eff}, of the disordered medium. ϵ_{eff} relates the averaged electric displacement field with the averaged electric field $\langle \mathbf{E} \rangle$. This is the mean-field description of the disordered media, where mean field is interpreted as the field in an effective uniform medium. However, from the knowledge of ϵ_{eff} it is not possible to obtain quadratic field

functions [41]. Although ϵ_{eff} does not fully characterize the light propagation in complex media, it can illuminate some aspects of the phenomenon as discussed below. ϵ_{eff} reads,

$$\epsilon_{ij}^{\text{eff}} = \epsilon_{ij} + i\zeta \sum_{l,n=x,y,z} (\delta_{ln} + \frac{i}{4} \sum_{k=x,y,z} e_{lnk} g_k) M_{il} M_{nj}\,, \qquad M_{il} = \delta_{il}(1 + a_l). \tag{5}$$

We use ϵ_{eff} to analyze the polarization eigenchannels in the system. For illustrative purposes, let us consider a simplified case when the direction of light propagation is parallel to the magnetization. There are two eigenchannels in the plane orthogonal to the gyration direction. They can be clearly presented in the Stokes parameters space,

$$q = E_x E_x^* - E_y E_y^*,\ u = E_x E_y^* + E_y E_x^*,\ v = i(E_x E_y^* - E_y E_x^*)\,, \tag{6}$$

by points on the Poincaré sphere [11] (see Figure 2a). In the non-magnetic medium, $\mathbf{g} = 0$, with an arbitrary value of anisotropy, $a \neq 0$, the light polarizations of eigenchannels are linear (blue points). For the opposite case, $\mathbf{g} \neq 0$ and $a = 0$, light polarizations are exactly circular (red points). Remarkably, for the general case of the magnetic medium with anisotropic inclusions, $\mathbf{g} \neq 0$ and $a \neq 0$, the polarization of eigenchannels is elliptical (purple points). Moreover, one can manipulate the polarizations by changing the ratio of the gyration, g, and the anisotropy, a. For example, if they are experimentally feasible when the gyration decreases for a fixed anisotropy, then the polarization smoothly changes from an elliptic to the linear one. This is depicted by purple line in Figure 2a.

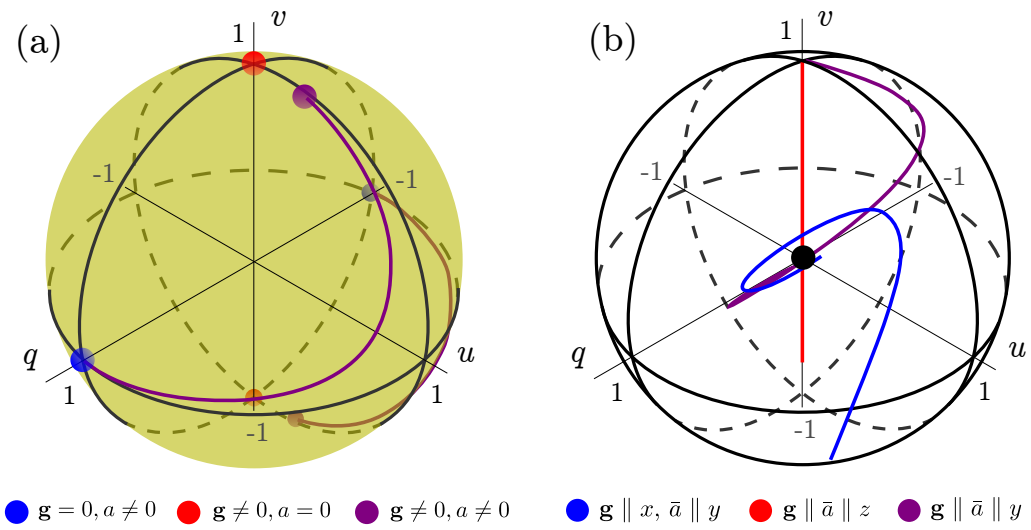

Figure 2. (**a**) Polarization eigenchannels for 3 types of disordered media are shown on the Poincaré sphere. They are depicted by blue dots for the non-magnetic case, $\mathbf{g} = 0$, with possible anisotropy, $a \neq 0$, corresponding to the linear polarization. For the magnetic case, $\mathbf{g} \neq 0$, without anisotropy, $a = 0$, they are depicted by red dots, corresponding to the circular polarization. For the general case, $\mathbf{g} \neq 0$, and for $a \neq 0$, they are depicted by purple dots, corresponding to the elliptical polarization. The modification of the polarization in the general case by manipulating the gyration is shown by purple lines. (**b**) Normalized Stokes parameters are computed for the electric field correlation matrix, $\tilde{W}(\mathbf{X})$, for components in the plane that is orthogonal to the gyration direction. Red line shows the oscillation of $\tilde{W}$ as a function of $\mathbf{X}$ for the case $\mathbf{g} \parallel \bar{a} \parallel z$. It is directed along the v-axis, so polarization oscillates between the right and left circularity, being limited to zero for a large value of $\mathbf{X}$ (the black dot, full depolarization) . For cases $\mathbf{g} \parallel \bar{a} \parallel y$ (purple curve) and $\mathbf{g} \parallel x$, $\bar{a} \parallel y$ (blue curve), symmetric contributions appear in the correlation. The polarizations acquire ellipticity, i.e., all Stokes parameters obtain non-zero values. (We assume that the direction of light propagation is parallel to the magnetization. $|\mathbf{g}| = 0.2$, $a = 0.1$)

3. Correlation Matrix

The observable quantity, which contains all the information about light propagation in the disordered medium, is the field correlation matrix $W_{kl}(\mathbf{r}, \mathbf{X})$ [11]:

$$W_{kl}(\mathbf{r}, \mathbf{X}) = \langle E_k(\mathbf{r}) E_l^*(\mathbf{r}') \rangle |_{\substack{\mathbf{r}=\mathbf{R}+\mathbf{X}/2+\mathbf{r}_0 \\ \mathbf{r}'=\mathbf{R}-\mathbf{X}/2+\mathbf{r}_0}}, \tag{7}$$

where $\mathbf{R} \equiv \frac{\mathbf{r}+\mathbf{r}'}{2} - \mathbf{r}_0$ is the distance between the light source and the observation area, and $\mathbf{X} \equiv \mathbf{r} - \mathbf{r}'$ is the distance between two observation points (see Figure 1). The computation of the field correlation matrix is the main goal of this work. It can be done by solving the Bethe–Salpeter equation in the ladder approximation for a far away source $2\pi l/R \ll 1$ [19].

Further, we use several approximations for the analytical derivation of the field correlation matrix. We restrict ourselves to the first-order contributions of the gyration and the anisotropy in the well-known diffusive approximation [42] (the largest term in the source distance, R, is considered). Thus, the following approximations were used:

$$\begin{gathered} \left(\frac{2\pi l}{R}\right)^2 \ll \frac{g}{\sqrt{\epsilon^0}\zeta} \ll \frac{2\pi l}{R} \ll 1, \\ \left(\frac{2\pi l}{R}\right)^2 \ll a \ll \frac{2\pi l}{R} \ll 1. \end{gathered} \tag{8}$$

Without a loss of a generality, let us assume that the observation axis (the radius–vector between the two detectors) is along the z-axis: $\mathbf{X} \parallel z$. The field correlation matrix is inversely proportional to the distance from the light source to the detectors, R. To analyze the electric field correlation, we use the normalized correlation matrix:

$$\begin{gathered} \tilde{\mathbf{W}}(\mathbf{X}) = \mathbf{W}(\mathbf{r}, \mathbf{X}) / \mathrm{Tr}[\mathbf{W}(\mathbf{r}, \mathbf{X} = 0)], \\ \mathrm{Tr}[\mathbf{W}(\mathbf{r}, \mathbf{X} = 0)] = (1 + \alpha)/8\pi^2 R l. \end{gathered} \tag{9}$$

Here, $\alpha = 10a/3$ when $\bar{a} \parallel z$ and $\alpha = -8a/3$ when $\bar{a} \perp z$.

The diagonal elements of the correlation matrix correspond to the correlations of electromagnetic fields with the same polarization. The magneto-optical effects do not affect these elements, unlike the anisotropy. In the absence of anisotropy, the correlations between light with polarizations perpendicular to the observation axis, W_{xx} and W_{yy}, are equal to each other but differ from the correlation parallel to the observation axis, W_{zz} [19]. In the presence of the anisotropy, two cases for diagonal elements of the correlation matrix are possible:

1. Anisotropy is along the observation axis ($\bar{a} \parallel z$). Correlations W_{xx} and W_{yy} are equal. Correlation W_{zz} is higher than W_{xx} and W_{yy} if $a > 0$ and vice versa.

$$\begin{gathered} \tilde{W}_{xx} = \tilde{W}_{yy} = \tilde{W}^0_{xx} + a(\tilde{W}^a_{xx} + \tilde{W}^a_{yy}), \\ \tilde{W}_{zz} = \tilde{W}^0_{zz} + 2a\tilde{W}^a_{zz}, \end{gathered} \tag{10}$$

where

$$\begin{gathered} \tilde{W}^0_{xx} = \frac{(\tilde{X}^2-1)\sin\tilde{X}+\tilde{X}\cos\tilde{X}}{2\tilde{X}^3}, \; \tilde{W}^0_{zz} = \frac{\sin\tilde{X}-\tilde{X}\cos\tilde{X}}{\tilde{X}^3}, \\ \tilde{W}^a_{xx} = -\frac{\tilde{X}(8\tilde{X}^2+27)\cos\tilde{X}+(5\tilde{X}^4+\tilde{X}^2-27)\sin\tilde{X}}{6\tilde{X}^5}, \\ \tilde{W}^a_{yy} = \frac{\tilde{X}(16\tilde{X}^2-81)\cos\tilde{X}+(7\tilde{X}^4-43\tilde{X}^2+81)\sin\tilde{X}}{6\tilde{X}^5}, \\ \tilde{W}^a_{zz} = \frac{(54-19\tilde{X}^2)\sin\tilde{X}+\tilde{X}(\tilde{X}^2-54)\cos\tilde{X}}{3\tilde{X}^5}, \end{gathered}$$

and $\tilde{X} = \sqrt{\epsilon^0} k_0 X$.

2. Anisotropy is perpendicular to the observation axis ($\bar{a} \perp z$). Correlations W_{xx} and W_{yy} are different. Correlation W_{yy} is higher than W_{xx} and W_{zz} if the anisotropy is along the y-axis and $a > 0$ and vice versa. The same is true if the anisotropy is along x as it corresponds to changing $W_{xx} \leftrightarrow W_{yy}$.

$$\begin{aligned} &\tilde{W}_{xx} = \tilde{W}^0_{xx} + a\tilde{W}^a_{xx}\,,\ \tilde{W}_{yy} = \tilde{W}^0_{xx} + a\tilde{W}^a_{yy}\,, \\ &\tilde{W}_{zz} = \tilde{W}^0_{zz} + a\tilde{W}^a_{zz}. \end{aligned} \tag{11}$$

The general rule here is that anisotropy $a > 0$ ($a < 0$) increases (decreases) the correlation of light with polarizations that are along the anisotropy axis. Additionally, the correlations perpendicular to the observation axis decrease slower than the parallel ones.

The off-diagonal correlation matrix elements correspond to the correlation of light with orthogonal polarizations. These elements are absent in the nonmagnetic medium. In the magnetic medium, there is a correlation of the electric field components perpendicular to the gyration. In the absence of anisotropy, the non-diagonal elements of the correlation matrix are anti-symmetric. This correlation decays faster when the gyration is perpendicular to the observation axis **X** than when the gyration is parallel to it [28]. In the presence of anisotropy, there are differences in the off-diagonal elements: $|W_{ij}| \neq |W_{ji}|$, $i \neq j$. The antisymmetric contribution, $\tilde{W}^A_\perp \equiv \frac{1}{2}(W_{ij} - W_{ji})(|\mathbf{g}|/\sqrt{\epsilon^0}\zeta)^{-1}$, varies weakly with the anisotropy, whereas the symmetric contribution, $\tilde{W}^S_\perp \equiv \frac{1}{2}(W_{ij} + W_{ji})(|\mathbf{g}|/\sqrt{\epsilon^0}\zeta)^{-1}$, appears.

This means that the light polarization acquires the elliptical part. We show it in the Stokes parameters space for the normalized correlation matrix (9). Stokes parameters are defined in the same way as in (6). For illustrative purposes, we restrict ourselves to the simplified case when the direction of light propagation is parallel to the magnetization, for example, in the case $\mathbf{g} \parallel z$: $q = \tilde{W}_{xx} - \tilde{W}_{yy}$, $u = \tilde{W}_{xy} + \tilde{W}_{yx}$, and $v = i(\tilde{W}_{xy} - \tilde{W}_{yx})$. Additionally, we normalize the vector (q, u, v) on its absolute value at $\mathbf{X} = 0$. In the case $\mathbf{g} \parallel \bar{a} \parallel z$, there is no symmetric contribution, and the polarization oscillates with distance $\mathbf{X} \parallel z$ from right to left circular polarization (red line along v-axis). For the case $\mathbf{g} \parallel \bar{a} \parallel y$, there is a small symmetric correlation part, oscillation mainly belongs to the (q-v)-plane (purple curve). A significant symmetric contribution appears for the case $\mathbf{g} \parallel x$, $\bar{a} \parallel y$ (blue curve). We note that the polarization correlation decreases with the increasing distance between the detectors. This fact reveals the attraction of the lines to the full depolarization point (black dot).

In the presence of gyration and anisotropy, five possibilities exist for the off-diagonal elements of the correlation matrix (for $\mathbf{X} \parallel z$):

1. The anisotropy is along the observation axis, while the gyration is perpendicular to both of them ($\mathbf{g} \perp \bar{a} \parallel z$) (Figure 3a,b). The symmetric contribution changes the correlations approximately by two times. The difference between these two figures is only in the sign of the symmetric part of the orthogonal correlations.

2. All three vectors are along the same axis ($\mathbf{g} \parallel \bar{a} \parallel z$) (Figure 3c). There is no symmetric contribution. The anti-symmetric contribution varies weakly with anisotropy.

3. All three vectors are perpendicular to each other ($\mathbf{g} \perp \bar{a} \perp z$) (Figure 3d). The symmetric contribution is of the same order as the anti-symmetric contribution.

4. The gyration is directed along the anisotropy but perpendicular to the observation axis ($\mathbf{g} \parallel \bar{a} \perp z$) (Figure 3e). The symmetric contribution exists, but it is small. The antisymmetric contribution varies weakly with anisotropy.

5. The gyration is along the observation axis, while the anisotropy is perpendicular to it ($\bar{a} \perp \mathbf{g} \parallel z$) (Figure 3f). The symmetric contribution is of the same order as the anti-symmetric one. The correlations decrease slowly in comparison with the case of $g \perp z$.

The explicit forms for the correlations of orthogonal polarizations are given in Appendix A.

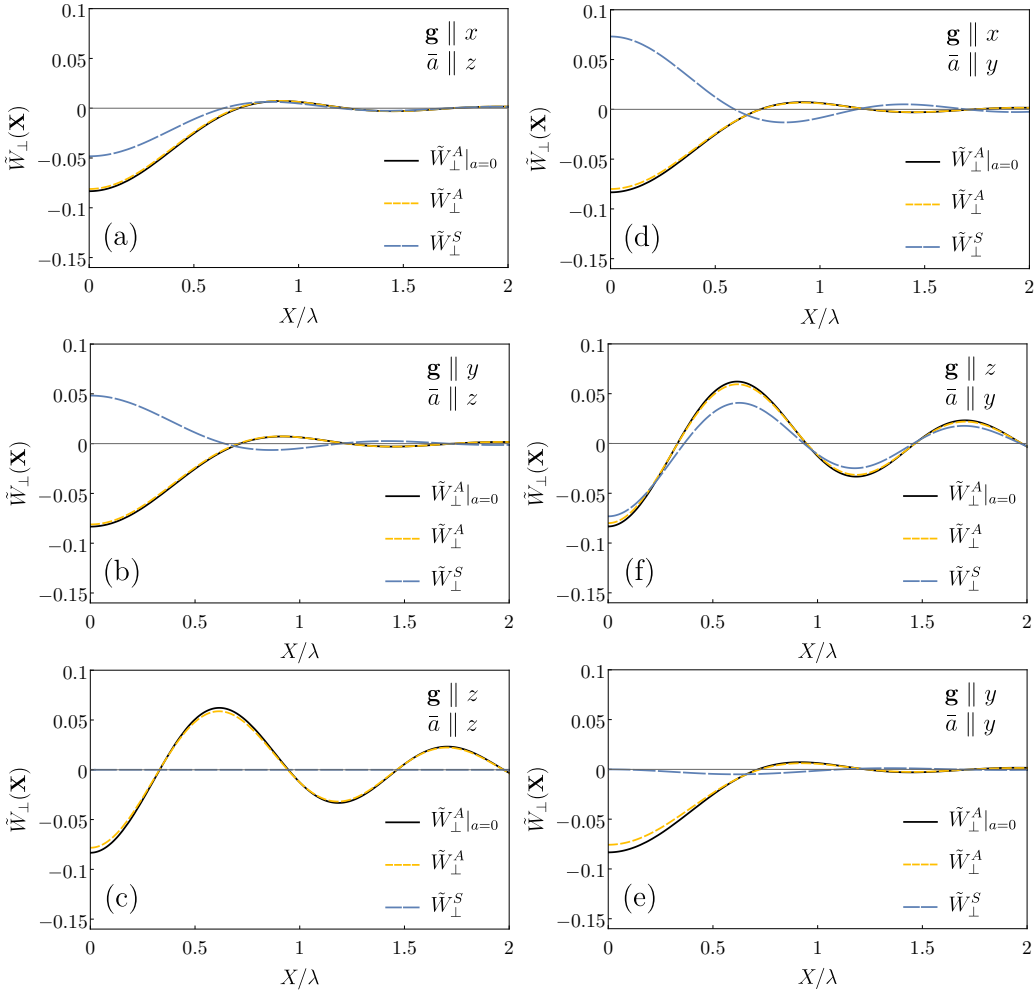

Figure 3. Symmetric $\tilde{W}_\perp^S$ and antisymmetric $\tilde{W}_\perp^A$ normalized contributions of the electric field correlations of the orthogonal polarizations for different directions of the gyration, $\mathbf{g}$, and the anisotropy, $\bar{a}$. Dependence on the gyration value $|\mathbf{g}|$ was included in the normalization factor. The anisotropy value is $a = 0.07$. Five different cases are possible (for $\mathbf{X} \parallel z$): (**a**) and (**b**) The anisotropy is along the observation axis, while the gyration is perpendicular to both of them; (**c**) All three vectors are along the same axis; (**d**) All three vectors are perpendicular to each other; (**e**) The gyration is directed along the anisotropy but perpendicular to the observation axis; (**f**) The gyration is along the observation axis, while the anisotropy is perpendicular to it.

4. Conclusions

We address the light-propagation problem in magnetic nanocomposites with oriented ellipsoidal scattering inclusions. Three cases are compared. In the magnetic media with spherical scatterers, an antisymmetric correlation of electromagnetic fields with orthogonal polarization is present. This corresponds to the rotation of polarization around the gyration vector, which does not depend on the initial polarization. In the non-magnetic media with oriented elliptical scatterers, there is only a correlation between electromagnetic fields with the same polarization. For the general case, in the magnetic scattering media with an anisotropy, an additional symmetric contribution of the correlation of electromagnetic fields with orthogonal polarizations appears. It corresponds to the elliptical polarization of transmission eigenchannels in these media. In such media, it is possible to manipulate the polarization by changing the medium gyration via an external magnetic field. By diminishing the gyration, one can reduce the circular and increase the linear contributions to the polarization of the scattered light. This effect has a non-additive character. That is, it is absent when either the gyration or the anisotropy are present. It arises only when the gyration and the anisotropy exist simultaneously.

Author Contributions: Supervision, V.I.B.; investigation R.A.N. and V.G.A. All authors have read and agreed to the published version of the manuscript.

Funding: The work was funded by RFBR, project numbers 19-32-60077 (R.A.N.) and 18-52-80038 (V.G.A. and V.I.B.).

Institutional Review Board Statement: Not applicable.

Informed Consent Statement: Not applicable.

Data Availability Statement: Not applicable.

Acknowledgments: We are grateful to Mikhail Kozhaev for his invaluable contribution to the article.

Conflicts of Interest: The authors declare no conflict of interest.

Appendix A

In this appendix, we explicitly write expressions for the correlations of orthogonal polarizations. In the presence of gyration and anisotropy, five cases for non-diagonal elements of the electric field correlation matrix (see Equation (9)) are possible (for $\mathbf{X} \parallel z$):

1. The anisotropy is along the observation axis, while the gyration is perpendicular to both of them ($\mathbf{g} \perp \bar{a} \parallel z$) (Figure 3a,b of the main text).

$$\begin{aligned}\tilde{W}_{\perp}^{A} &= \tilde{W}_{\perp}^{A(0,\perp)} + \frac{a((36-13\tilde{X}^2)\sin\tilde{X}+\tilde{X}(\tilde{X}^2-36)\cos\tilde{X})}{12\tilde{X}^5},\\ \tilde{W}_{\perp}^{S} &= \frac{3a((24-13\tilde{X}^2)\sin\tilde{X}+\tilde{X}(5\tilde{X}^2-24)\cos\tilde{X})}{4\tilde{X}^5},\\ \tilde{W}_{\perp}^{A(0,\perp)} &= \frac{(\tilde{X}\cos\tilde{X}-\sin\tilde{X})}{4\tilde{X}^3}\end{aligned} \tag{A1}$$

2. All of the three vectors are along the same axis ($\mathbf{g} \parallel \bar{a} \parallel z$) (Figure 3c of the main text).

$$\begin{aligned}\tilde{W}_{\perp}^{A} &= \tilde{W}_{\perp}^{A(0,\parallel)} + \frac{a((\tilde{X}^4+13\tilde{X}^2-36)\sin\tilde{X}-\tilde{X}(\tilde{X}^2-36)\cos\tilde{X})}{6\tilde{X}^5},\\ \tilde{W}_{\perp}^{S} &= 0,\\ \tilde{W}_{\perp}^{A(0,\parallel)} &= \frac{((2-\tilde{X}^2)\sin\tilde{X}-2\tilde{X}\cos\tilde{X})}{4\tilde{X}^3}.\end{aligned} \tag{A2}$$

3. All of the three vectors are perpendicular to each other ($\mathbf{g} \perp \bar{a} \perp z$) (Figure 3d of the main text).

$$\begin{aligned}\tilde{W}_{\perp}^{A} &= \tilde{W}_{\perp}^{A(0,\perp)} - \frac{a((9-5\tilde{X}^2)\sin\tilde{X}+\tilde{X}(2\tilde{X}^2-9)\cos\tilde{X})}{12\tilde{X}^5},\\ \tilde{W}_{\perp}^{S} &= -\frac{a(3(44-21\tilde{X}^2)\sin\tilde{X}+\tilde{X}(19\tilde{X}^2-132)\cos\tilde{X})}{4\tilde{X}^5}.\end{aligned} \tag{A3}$$

4. The gyration is directed along the anisotropy but perpendicular to the observation axis ($\mathbf{g} \parallel \bar{a} \perp z$) (Figure 3e of the main text).

$$\begin{aligned}\tilde{W}_{\perp}^{A} &= \tilde{W}_{\perp}^{A(0,\perp)} - \frac{a((27-14\tilde{X}^2)\sin\tilde{X}+\tilde{X}(5\tilde{X}^2-27)\cos\tilde{X})}{12\tilde{X}^5},\\ \tilde{W}_{\perp}^{S} &= -\frac{a(3(5-2\tilde{X}^2)\sin\tilde{X}+\tilde{X}(\tilde{X}^2-15)\cos\tilde{X})}{\tilde{X}^5}.\end{aligned} \tag{A4}$$

5. The gyration is along the observation axis, while the anisotropy is perpendicular to it ($\bar{a} \perp \mathbf{g} \parallel z$) (Figure 3f of the main text).

$$\begin{aligned}\tilde{W}_{\perp}^{A} &= \tilde{W}_{\perp}^{A(0,\parallel)}\\ &\quad + \frac{a(\tilde{X}(7\tilde{X}^2-36)\cos\tilde{X}+(2\tilde{X}^4-19\tilde{X}^2+36)\sin\tilde{X})}{12\tilde{X}^5},\\ \tilde{W}_{\perp}^{S} &= -\frac{a(2\tilde{X}(11\tilde{X}^2-39)\cos\tilde{X}+3(3\tilde{X}^4-16\tilde{X}^2+26)\sin\tilde{X})}{4\tilde{X}^5}.\end{aligned} \tag{A5}$$

References

1. Berne, B.J.; Pecora, R. *Dynamic Light Scattering: With Applications to Chemistry, Biology, and Physics*; Courier Corporation: Chelmsford, MA, USA, 2000.
2. Brongersma, M.L.; Kik, P.G. *Surface Plasmon Nanophotonics*; Springer: Berlin/Heidelberg, Germany, 2007.
3. Skipetrov, S.E. Optical devices: Localizing light with electrons. *Nat. Nanotechnol.* **2014**, *9*, 335. [CrossRef] [PubMed]
4. Réfrégier, P.; Wasik, V.; Vynck, K.; Carminati, R. Analysis of coherence properties of partially polarized light in 3D and application to disordered media. *Opt. Lett.* **2014**, *39*, 2362. [CrossRef] [PubMed]
5. Wang, Y.; Yan, S.; Kuebel, D.; Visser, T.D. Dynamic control of light scattering using spatial coherence. *Phys. Rev. A* **2015**, *92*, 013806. [CrossRef]
6. Gorodnichev, E.E.; Kuzovlev, A.I.; Rogozkin, D.B. Impact of wave polarization on long-range intensity correlations in a disordered medium. *J. Opt. Soc. Am. A* **2016**, *33*, 95–106. [CrossRef] [PubMed]
7. Hoskins, J.G.; Schotland, J.C. Acousto-optic effect in random media. *Phys. Rev. E* **2017**, *95*, 033002. [CrossRef]
8. Uchida, H.; Masuda, Y.; Fujikawa, R.; Baryshev, A.; Inoue, M. Large enhancement of Faraday rotation by localized surface plasmon resonance in Au nanoparticles embedded in Bi: YIG film. *J. Magn. Magn. Mater.* **2009**, *321*, 843–845. [CrossRef]
9. Strudley, T.; Akbulut, D.; Vos, W.L.; Lagendijk, A.; Mosk, A.P.; Muskens, O.L. Observation of intensity statistics of light transmitted through 3D random media. *Opt. Lett.* **2014**, *39*, 6347–6350. [CrossRef]
10. de Aguiar, H.B.; Gigan, S.; Brasselet, S. Polarization recovery through scattering media. *Sci. Adv.* **2017**, *3*, e1600743. [CrossRef]
11. Dogariu, A.; Carminati, R. Electromagnetic field correlations in three-dimensional speckles. *Phys. Rep.* **2015**, *559*, 1–29. [CrossRef]
12. Wolf, E. Unified theory of coherence and polarization of random electromagnetic beams. *Phys. Lett. A* **2003**, *312*, 263–267. [CrossRef]
13. Wolf, E. Correlation-induced changes in the degree of polarization, the degree of coherence, and the spectrum of random electromagnetic beams on propagation. *Opt. Lett.* **2003**, *28*, 1078. [CrossRef] [PubMed]
14. Jonckheere, T.; Müller, C.A.; Kaiser, R.; Miniatura, C.; Delande, D. Multiple scattering of light by atoms in the weak localization regime. *Phys. Rev. Lett.* **2000**, *85*, 4269. [CrossRef] [PubMed]
15. Wiersma, D.S.; Bartolini, P.; Lagendijk, A.; Righini, R. Localization of light in a disordered medium. *Nature* **1997**, *390*, 671–673. [CrossRef]
16. Lagendijk, A.; van Tiggelen, B.; Wiersma, D.S. Fifty years of Anderson localization. *Phys. Today* **2009**, *62*, 24–29. [CrossRef]
17. Segev, M.; Silberberg, Y.; Christodoulides, D.N. Anderson localization of light. *Nat. Photonics* **2013**, *7*, 197–204. [CrossRef]
18. Sperling, T.; Schertel, L.; Ackermann, M.; Aubry, G.J.; Aegerter, C.M.; Maret, G. Can 3D light localization be reached in 'white paint'? *New J. Phys.* **2016**, *18*, 013039. [CrossRef]
19. Vynck, K.; Pierrat, R.; Carminati, R. Polarization and spatial coherence of electromagnetic waves in uncorrelated disordered media. *Phys. Rev. A* **2014**, *89*, 013842. [CrossRef]
20. Vynck, K.; Pierrat, R.; Carminati, R. Multiple scattering of polarized light in disordered media exhibiting short-range structural correlations. *Phys. Rev. A* **2016**, *94*, 033851. [CrossRef]
21. Rikken, G.; Van Tiggelen, B. Observation of magnetically induced transverse diffusion of light. *Nature* **1996**, *381*, 54–55. [CrossRef]
22. Erbacher, F.; Lenke, R.; Maret, G. Multiple light scattering in magneto-optically active media. *Europhys. Lett.* **1993**, *21*, 551. [CrossRef]
23. Skipetrov, S.; Sokolov, I. Magnetic-field-driven localization of light in a cold-atom gas. *Phys. Rev. Lett.* **2015**, *114*, 053902. [CrossRef] [PubMed]
24. Golubentsev, A.A. Interference correction to the albedo of a strongly gyrotropic medium with random inhomogeneities. *Radiophys. Quantum Electron.* **1984**, *27*, 506–516. [CrossRef]
25. MacKintosh, F.C.; John, S. Coherent backscattering of light in the presence of time-reversal-noninvariant and parity-nonconserving media. *Phys. Rev. B* **1988**, *37*, 1884–1897. [CrossRef] [PubMed]
26. van Tiggelen, B.A.; Maynard, R.; Nieuwenhuizen, T.M. Theory for multiple light scattering from Rayleigh scatterers in magnetic fields. *Phys. Rev. E* **1996**, *53*, 2881–2908. [CrossRef]
27. Niyazov, R.A.; Kozhaev, M.A.; Achanta, V.G.; Belotelov, V.I. Polarization Eigenchannels in a Magnetic Uncorrelated Disordered Medium. *Phys. Met. Metallogr.* **2022**, *123*, 447–450. [CrossRef]
28. Kozhaev, M.A.; Niyazov, R.A.; Belotelov, V.I. Correlation of light polarization in uncorrelated disordered magnetic media. *Phys. Rev. A* **2017**, *95*, 023819. [CrossRef]
29. Mittal, M.; Furst, E.M. Electric Field-Directed Convective Assembly of Ellipsoidal Colloidal Particles to Create Optically and Mechanically Anisotropic Thin Films. *Adv. Funct. Mater.* **2009**, *19*, 3271–3278. [CrossRef]
30. Li, Z.Y.; Wang, J.; Gu, B.Y. Creation of partial band gaps in anisotropic photonic-band-gap structures. *Phys. Rev. B* **1998**, *58*, 3721–3729. [CrossRef]
31. Sadecka, K.; Gajc, M.; Orlinski, K.; Surma, H.B.; Klos, A.; Jozwik-Biala, I.; Sobczak, K.; Dluzewski, P.; Toudert, J.; Pawlak, D.A. When Eutectics Meet Plasmonics: Nanoplasmonic, Volumetric, Self-Organized, Silver-Based Eutectic. *Adv. Opt. Mater.* **2014**, *3*, 381–389. [CrossRef]
32. Grzelczak, M.; Vermant, J.; Furst, E.M.; Liz-Marzán, L.M. Directed Self-Assembly of Nanoparticles. *ACS Nano* **2010**, *4*, 3591–3605. [CrossRef]

33. Ding, T.; Song, K.; Clays, K.; Tung, C.H. Fabrication of 3D Photonic Crystals of Ellipsoids: Convective Self-Assembly in Magnetic Field. *Adv. Mater.* **2009**, *21*, 1936–1940. [CrossRef]
34. Khramova, A.E.; Ignatyeva, D.O.; Kozhaev, M.A.; Dagesyan, S.A.; Berzhansky, V.N.; Shaposhnikov, A.N.; Tomilin, S.V.; Belotelov, V.I. Resonances of the magneto-optical intensity effect mediated by interaction of different modes in a hybrid magneto-plasmonic heterostructure with gold nanoparticles. *Opt. Express* **2019**, *27*, 33170. [CrossRef] [PubMed]
35. Wolf, E. Optics in terms of observable quantities. *Il Nuovo C. (1943-1954)* **1954**, *12*, 884–888. [CrossRef]
36. Roychowdhury, H.; Wolf, E. Determination of the electric cross-spectral density matrix of a random electromagnetic beam. *Opt. Commun.* **2003**, *226*, 57–60. [CrossRef]
37. Born, M.; Wolf, E. *Principles of Optics: 60th Anniversary Edition*, 7 ed.; Cambridge University Press: Cambridge, UK, 2019. [CrossRef]
38. Sheng, P. *Introduction to Wave Scattering, Localization and Mesoscopic Phenomena*; Springer Science & Business Media: Berlin/Heidelberg, Germany, 2006; Volume 88.
39. Akkermans, E.; Montambaux, G. *Mesoscopic Physics of Electrons and Photons*; Cambridge University Press: Cambridge, UK, 2007.
40. Bharucha-Reid, A. *Probabilistic Methods in Applied Mathematics*; Elsevier Science: Amsterdam, The Netherlands, 2014; Volume 3.
41. Brekhovskikh, V.L. Effective dielectric constant in the calculation of the second field moments in a randomly inhomogeneous medium. *Zh. Eksp. Teor. Fiz* **1985**, *89*, 2013–2020.
42. van Rossum, M.C.W.; Nieuwenhuizen, T.M. Multiple scattering of classical waves: Microscopy, mesoscopy, and diffusion. *Rev. Mod. Phys.* **1999**, *71*, 313–371. [CrossRef]